Vehicle Dynamics Modeling for Autonomous Racing Using Gaussian Processes

Jingyun Ning
Dept. of Electrical and Computer Engineering
Univ. of Virginia
jn2ne@virginia.edu

Madhur Behl
Dept. of Computer Science
Univ. of Virginia
madhur.behl@virginia.edu

arXiv:2306.03405v1 [cs.RO] 6 Jun 2023

Abstract: Autonomous racing is increasingly becoming a proving ground for autonomous vehicle technology at the limits of its current capabilities. The most prominent examples include the F1Tenth racing series, Formula Student Driverless (FSD), Roborace, and the Indy Autonomous Challenge (IAC). Especially necessary, in high speed autonomous racing, is the knowledge of accurate racecar vehicle dynamics. The choice of the vehicle dynamics model has to be made by balancing the increasing computational demands in contrast to improved accuracy of more complex models. Recent studies have explored learning-based methods, such as Gaussian Process (GP) regression for approximating the vehicle dynamics model. However, these efforts focus on higher level constructs such as motion planning, or predictive control and lack both in realism and rigor of the GP modeling process, which is often over-simplified. This paper presents the most detailed analysis of the applicability of GP models for approximating vehicle dynamics for autonomous racing. In particular we construct dynamic, and extended kinematic models for the popular F1TENTH racing platform. We investigate the effect of kernel choices, sample sizes, racetrack layout, racing lines, and velocity profiles on the efficacy and generalizability of the learned dynamics. We conduct 400+ simulations on real F1 track layouts to provide comprehensive recommendations to the research community for training accurate GP regression for single-track vehicle dynamics of a racecar.

1 Introduction

The rising popularity of self-driving cars has led to the emergence of a new research field in recent years: Autonomous racing. Researchers are developing algorithms for high-performance race vehicles which aim to operate autonomously on the edge of the vehicle's limits: High speeds, high accelerations, low reaction times, highly uncertain, dynamic, and adversarial environments. Competitions in autonomous racing have been held not only in simulators [1, 2], but also on hardware with racecars' ranging from 1:43 scale RC cars [3] to 1/10 scale (F1tenth Racing [4]) to full size Indy racecars [5].

The modeling of the vehicle dynamics behavior of the racecar is an essential part in the field of autonomous racing. The current state of the art provides many variations of vehicle dynamics modeling such as single track model, double track model or full vehicle model. The more complicated the vehicle dynamics model, the more parameters are needed. Unfortunately not all of those parameters are available in detail for a vehicle and so different methods for estimating these parameters are proposed - especially for nonlinear vehicle parameters like the tires. A major challenge is the model mismatch between mathematical model and real vehicle dynamics. While researches in vehicle modeling have developed several models, from simplest point-mass model to fully multi-body model [6, 7], the modeling errors are inevitable due to highly non-linearity of real vehicle dynamics.

Consequentially, implementation of learning-based methods to compensate the error between simulation models and real vehicle models has received attention from researchers. Gaussian Processes

Notations	Vehicle Dynamics		
x,y: vehicle position w.r.t. inertial frame	Kinematic	Dynamic	E-Kin
v: Velocity $[m/s]$	$\dot{x} = v\cos(\psi)$	$\dot{x} = v\cos(\psi + \beta)$	$\dot{x} = v\cos(\psi + \beta)$
δ: Steering angle $[rad]$	$\dot{y} = v\sin(\psi)$	$\dot{y} = v\sin(\psi + \beta)$	$\dot{y} = v\sin(\psi + \beta)$
ψ: Heading angle $[rad]$	$\dot{\delta} = v_\delta$	$\dot{\delta} = v_\delta$	$\dot{\delta} = v_\delta$
ω: Yaw rate $[rad/s]$	$\dot{v} = a_{long}$	$\dot{v} = a_{long} = \frac{F_{rx}}{m}$	$\dot{v} = a_{long}$
β: Body slip angle $[rad]$	$\dot{\psi} = \frac{v}{l_r+l_f}\tan(\delta)$	$\dot{\psi} = \omega = \frac{v}{l_r+l_f}\tan(\delta)$	$\dot{\psi} = \omega$
a_{long}: Longitudinal acceleration $[m/s^2]$		$\dot{\omega} = \frac{1}{I_z}(l_f F_{fy}\cos\delta_f - l_r F_{ry})$	$\dot{\omega} = \frac{1}{l_r+l_f}(\dot{\delta}v + \delta\dot{v})$
δ_v: Steering velocity $[rad/s]$		$\dot{\beta} = \frac{1}{mv}(F_{fy} + F_{ry}) - \omega$	$\dot{\beta} = (l_r + l_f)(\dot{\delta}v + \delta\dot{v})$

Table 1: Mathematical descriptions of different vehicle dynamics models

(GP) based models are powerful candidates among such methods. Previous work [8] on autonomous racing has explored implementing GP regression for vehicle dynamics modeling. However, their exploration is limited and lacks rigorous analysis - such as knowledge of GP model kernel selection, sample size, different racing lines and track layouts. During GP model selection, both the form of the mean function and covariance kernel function need to be carefully chosen and tuned. While the mean function is typically constant, either zero or the mean of the training dataset. There are many options for the covariance kernel functions: they can have many forms as long as it follows the properties of a kernel. Moreover, autonomous racing specific criteria such as vehicle velocity profiles and racetrack curviness are often omitted when implementing GP for vehicle modeling.

This paper presents the most detailed analysis of the suitability of GPs for vehicle dynamics modeling for autonomous racing to date. We build a dynamic and extended kinematic (E-Kin) model of the 1/10 scale racecar using a realistic simulation platform (F1TENTH Gym). In addition, we provide a comprehensive study for GP model selection based on:

1. Vehicle dynamics model in three real-world Formula One racetracks: Shanghai International Circuit, Sepang International Circuit, and Yas Marina Circuit.
2. Different driving scenarios combinations: Different velocity profiles and racelines during the data collection and their effect on GP accuracy.
3. Exploration of suitable combinations of five GP kernel functions.
4. Analysis of the effect of training sample size on the model accuracy.

To answer the above questions, we provide a comprehensive and rigorous analysis of GPs for vehicle dynamic modeling by conducting 400+ simulations.

2 Background: Vehicle Dynamics Modeling

We consider the single-track model in this paper, in which the two front wheels as well as the two rear wheels are lumped into one wheel each. Both kinematic model and dynamic model has been described in this section. Following simplifications have been made: (i) we assume the vehicle to have planar motion, (ii) as the car used is rear wheel driven, the longitudinal force on the front wheel is neglected.

2.1 Kinematic single-track model

Kinematic single-track model is preferred in applications for its simplicity [9, 10]. We adopt the kinematic model from [11].

The kinematic model requires two tuning parameters, l_r and l_f, which represent the distance from center of gravity (C.O.G.) to the rear and front axles, respectively. The differential equations for such a model are given in Table 1. x and y are the location of C.O.G. with respect to the inertial frame.

Velocity at the C.O.G. of the vehicle is denoted by v. Ψ is vehicle inertial heading orientation, and a_{long} is longitudinal acceleration. δ is steering angle represents the angle between vehicle heading and front wheel direction.

2.2 Single-track model

At higher speeds, kinematic models can not be applied since they do not consider tire slip, which means important effects such as understeer or oversteer are not considered [12]. Therefore, when performing planning of evasive maneuvers closer to physical limits, a single-track (dynamic) model needs to be developed for both lateral and longitudinal control [13, 14], shown in Fig. 1. The slip angle of a tire is defined as the angle between the orientation of the tire and the orientation of the velocity vector of the wheel. The mathematical descriptions are denoted in Table 1, where

$$F_{yf} = 2\mu C_{sf} \frac{(mgl_r - ma_{long}h_{cog})}{l_f + l_r} \alpha_f \tag{1a}$$

$$F_{yr} = 2\mu C_{sr} \frac{(mgl_f + ma_{long}h_{cog})}{l_f + l_r} \alpha_r \tag{1b}$$

$$\alpha_f = \delta - \beta - \frac{l_f \omega}{v} \tag{2a}$$

$$\alpha_r = (-\beta + \frac{l_r \omega}{v}) \tag{2b}$$

F_{rx} is the longitudinal force at the rear axle, and F_{fy}, F_{ry} are the lateral forces at front axle and rear axle, respectively. Their governing equations are described as (1a) and (1b), where α_f and α_r are tire slip angles at front wheels and rear wheels, respectively.

2.3 Extended kinematic model

A well-tuned single-track model is suitable for autonomous racing with advanced control algorithms. However, due to the model complexity, the model tuning procedure is time prohibitive. In addition, we need access to the tire models for calculating lateral forces, and the tire models need to be recalibrated each time for a new racetrack, which increases the cost of implementing such a dynamic model. While a simpler kinematic model is enough for low-speed driving behaviors, the model mismatch will become significant at much higher speeds.

Therefore, in this work, we adopt learning-based extended kinematic (E-Kin) model, which has same states as a dynamic model, and we use GP models to calculate the discrepancies between models. Mathematical representation is shown in Table 1. The differences between E-kin and dynamic model lie in yaw rate, ω, and vehicle body slip angle, β, as shown in Eq. 3.

$$\dot{\omega} = \frac{1}{l_r + l_f}(\dot{\delta} v + \delta \dot{v}) \tag{3a}$$

$$\dot{\beta} = (l_r + l_f)(\dot{\delta} v + \delta \dot{v}) \tag{3b}$$

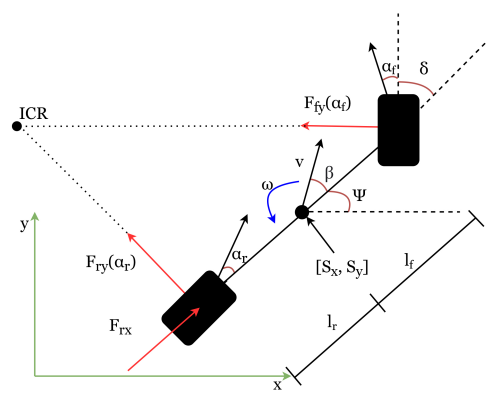

Figure 1: Single-track dynamic vehicle model. Reference point: C.O.G.

3 Related Work

GP regression models have become popular for autonomous driving in the past decade, especially in

autonomous racing. They can be implemented to predict ego and target vehicle behaviors in multi-agent scenarios when the ego vehicle performs an overtake maneuver.

The work of Hewing et al makes use of a sparse GP approximation with dynamically adjusting inducing inputs and enable a real-time implementable NMPC controller to increase the racing performance. This method aims to learn from vehicle sensor data with GP to improve the ego vehicle dynamics model [15].

Wischnewski et al. [16] present the implementation of GP for a nonlinear regression problem. This approach tends to mitigate the gap between planned and driven trajectory which is caused by the control system quality and unmodelled effects.

[17, 18] use GP models to predict future target vehicle behaviors in a head-to-head racing environment. Those work employs the GP models to predict target vehicle trajectories learned from previous behaviors for ego vehicles to decide whether to perform overtaking maneuvers or not.

The extended kinematic model in this paper is inspired by Jain et al. [8]. In their work, they utilized the GP regression model to identify uncertainties between the extended kinematic and dynamic models and demonstrated the capability of MPC implementation on their extended kinematic model.

All of the related work have utilized GP models for either predicting target vehicle trajectories or identifying errors of ego vehicle states from a simpler vehicle model. However, they are limited in following aspects:

1. The lack of knowledge of GPs kernel function selection;
2. The impact on different sample sizes for training GPs;
3. The effect of utilizing different racing lines and speed profiles;
4. Racetracks are not realistic.

4 Problem Statement

4.1 List of Assumptions

4.1.1 Assumption 1: 2D planar

This paper assumes the vehicle is driving in two-dimensional space, i.e., only yaw angles are being considered. In the future, this assumption can be relaxed by selecting racetracks that have banked curves, which will introduce the pitch angles in addition to yaw angles.

4.1.2 Assumption 2: Full knowledge of the vehicle model

We use a single-track dynamic model to represent the real vehicle model and assume that the F1TENTH Gym data of the dynamic model corresponds to the ground truth. This simplification can be relaxed by either implementing a more sophisticated vehicle model, e.g., a multi-body vehicle model, or using a realistic simulator, e.g., an SVL simulator.

4.1.3 Assumption 3: Perfect sensor measurements

The racecar in the F1TENTH Gym simulator includes on-board LIDAR and IMU, which can estimate the wheel odometry. This paper assumes the vehicle has sufficient sensors to measure the states of interest for training GPs, and there are no sensor noises associated with data collection. This assumption could be relaxed in the future by introducing random noises to the sensor measurements.

4.2 Problem formulation

In this paper, we have not only built a dynamic model and extended kinematic model of the F1TENTH racecar, but also trained GP regression model to learn the mismatch between these models. We build

the corrected kinematic model, f_{corr}, as an approximation of the dynamic model:

$$f_{dyn} \sim f_{corr} \tag{4}$$

where the corrected model is a combination of E-kin model, f_{E-Kin}, and error model, e.

$$f_{corr}(x_k, u_k) = f_{E-Kin}(x_k, u_k) + e(x_k, u_k) \tag{5}$$

We define the form of error model in Eq. 6:

$$e(x_k, u_k) = x_{k+1} - f_{E-Kin}(x_k, u_k) \tag{6}$$

x is the vehicle sensor measurements (states), consists of: $[X, Y, v, \omega, \beta]$, u is control inputs, which are $[a_{long}, \delta_v]$, and f_{E-Kin} is the estimates which are calculated by the E-Kin model. Since the model mismatches are only in the yaw rate ω, and body slip angle, β, we define the formula of GP learned error model as in 7.

$$e = \mathcal{GP}(\omega, \beta, a, \delta_v) \tag{7}$$

In the next section, we will describe the methods of generating the data set for GP to learn the error models.

5 Methodologies

5.1 Model selection

The goal of our method is to explore the best setting for training GPs for vehicle dynamic modeling in autonomous racing. In other words, we want to evaluate the effect of different kernel functions, sample sizes, racing scenarios and racetrack layouts on training GP models.

For the model selection, we design workflow as depicted in Fig 2: For each Formula One tracks, we collect training data of four different racing scenarios with different sample sizes. Then we train GP models with different combinations of five standard kernel functions. Thus, to decide the best model setting, we have conducted a thorough $3 \times 4 \times 3 \times 12 = 432$ experiments. The details of model schemes analysis are shown in Table 3.

5.2 Kernel composing

Kernel composing is the standard method for training GP models with more than one type of feature. [19]. Since the GP models learned in this paper has different features of input data, acceleration, a_{long} and steering velocity, δ_v. We have selected five standard kernel functions, Table 2, to explore the effect of different kernel composing on training GP models. The multiplication and addition are denoted as following

5.3 Racing scenarios

The choices of race line and velocity profiles also influence GP accuracy. Therefore, in the evaluation, we have composed four racing scenarios containing the combinations of these factors.

5.3.1 RA_NON-CAP

The vehicle is driving on track to follow an optimal raceline, plus no fixed speed reference to limit the outputs of the pure pursuit controller. In other words, when driving through a long straight track sector, the vehicle will be available to perform a linear speed change of acceleration or deceleration. See in Fig. 3b

Standard Kernel Functions	Mathematical Definition
RBF	$k_{RBF}(x,x') = \sigma^2 \mathbf{exp}(-\frac{(x-x')^2}{2l^2})$
RQ	$k_{RQ}(x,x') = \sigma^2(1+\frac{(x-x')^2}{2\alpha l^2})$
PERIODIC	$k_{PER}(x,x') = \sigma^2 \mathbf{exp}(-\frac{2sin^2(\pi\lvert x-x'\rvert/p)}{l^2})$
LINEAR	$k_{LIN}(x,x') = \sigma_b^2 + \sigma_v^2(x-c)(x'-c)$
MATERN	$k_{MAT}(x,x') = \frac{1}{\Gamma(v)2^{\nu-1}}(\frac{\sqrt{2\nu}}{l}d(x,x'))^{\nu}K_{\nu}(\frac{\sqrt{2\nu}}{l}d(x,x'))$

Table 2: Standard kernel functions and math definition.

Sample Number	V profiles	Race line	Tracks	Kernels functions	Kernel combinations
Full size	Capped	Center line	Shanghai	RBF	$k_{RBF} + (k_{PER}, k_{LIN})$
				PERIODIC	$k_{RQ} + (k_{PER}, k_{LIN})$
Half size			Sepang	RQ	$k_{MAT} + (k_{PER}, k_{LIN})$
	Non-capped	Race line		LINEAR	$k_{RBF} \times k_{RQ}$
1/3 size			Yas Marina	MATERN	$k_{MAT} \times (k_{PER}, k_{RBF}, k_{LIN})$
					$k_{RQ} \times (k_{LIN}, k_{MAT})$

Table 3: In-depth analysis of GP model schemes.

5.3.2 CE_NON-CAP

The vehicle is driving to follow the center line of each track. The purpose is to compare the GP performances between optimal raceline and simple center line to investigate the importance of calculating raceline in GP model training.

5.3.3 RA_CAP

The vehicle is driving along the optimal raceline as mentioned before but with a fixed reference speed. This will limit the vehicle's top speed in a long straight trajectory. Sometimes a predefined speed profile is not easily accessible with each given track, and it can be non-trivial to create. We design this scenario to show if the GP model performance will decrease when the vehicle is only driving under a fixed speed reference.

5.3.4 CE_CAP

The vehicle is driving on the center line with a fixed speed reference. We compare this scenario with both RA_CAP and CE_NON-CAP. Thus, we can comprehensively analyze the importance of both speed and raceline profiles in the GP model training process.

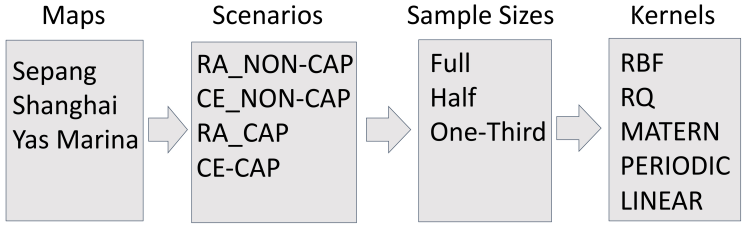

Figure 2: Workflow of exploring the best settings for GP training for vehicle dynamic modeling.

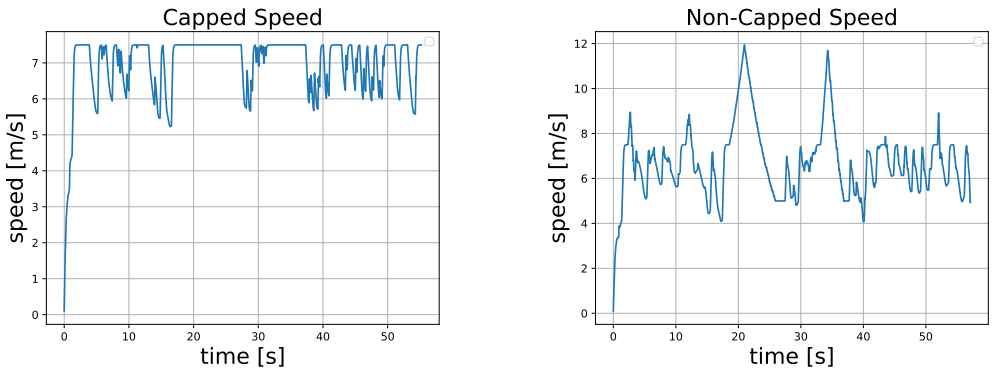

(a) (b)

Figure 3: Velocity profiles: (a) Capped by a fixed reference speed (e.g. $7.5[m/s]$); (b) Non-capped speed, dynamic reference speed profile, has linear acceleration and deceleration when driving on straight lines.

5.4 Sample sizes in Gaussian Process

Since GP regression is a non-parametric method, it needs to consider the whole training data each time when making a prediction. This characteristic brings the most prominent weakness of GP: it is computationally expensive. Because of the inversion and determinant of the nn kernel matrix $K(X, X)$, GP suffers from a cubic time complexity $\mathcal{O}(n^3)$, which limits the scalability of GP. With the inspiration of [20], we evaluate the benefits of two types of scalable GPs for vehicle modeling: (1) Global approximations approximate the kernel function through global distillation. Specifically, we divide the size of training sample (n) into three categories: (i) full size, (ii) half size, and (iii) one-third of full size. (2) Local approximations follow the idea of divide-and-conquer to focus on the local subsets of training data. We divide racetrack into three sectors based on their characteristics and approximate the kernel function through each sector. We test our sector-based GP on the whole track dataset.

6 Experiment Setup

6.1 Simulation setup

6.1.1 F1TENTH Gym

As shwon in Fig. 4, is created for research that needs an asynchronous, realistic vehicle simulation with multiple vehicle instances in the same environment [21]. This simulator provides a lightweight, 2D-simulation with an openAI Gym interface. We use ROS2 based F1TENTH Gym as the simulator platform, and all of the simulations are conducted in Unbuntu 20.04.3 LTS operating system, with an Intel Core i7-10700K CPU.

In addition, unlike previous work, where researchers made up the racetracks. This paper conduct the experiments on three realistic Formula One racetracks, as shown in Fig. 4, which are: (i) Sepang International Circuit; (ii) Shanghai International Circuit; (iii) Yas Marina Circuit.

6.2 Data collection

We treat the F1tenth Gym environment as the ground truth vehicle dynamics. The model used in the Gym environment is a single-track model from [11]. Thus, we use the collected measurements from Gym environment to address the model mismatch.

The data set has two components, see Table 1: (i) Vehicle states: $[x, y, v, \omega, \beta]$; (ii) Control inputs: $[a_{long}, \delta_v]$. We collect data by implementing a pure pursuit controller [22] in F1TENTH gym

environment. For each racetrack, we compute the optimal raceline [23] and then track it using the pure pursuit controller. We collect data at a frequency of 60Hz in the form of state-action-state pairs. Dynamic data is denoted by $\mathcal{D}_{dyn} = \{x_k, u_k, x_{k+1}\}, \forall k \in \{0, 1, ..T-1\}$, where T is the number of data sample size.

6.3 Training process

To address the data mismatch between dynamic and E-Kin model data, we use the collected $\mathcal{D}_{dyn}$. Since the parameters of the E-Kin model f_{kin} are known, we generate a new dataset $\mathcal{D}_{kin}$ that captures its response when excited with the same inputs starting from the same initialization. $D_{kin} = \{x_t, u_t, f_{kin}(x_t, u_t)\}, \forall k \in \{0, 1, ..T-1\}$, where x_k, u_k are states and control inputs data from D_{dyn}. Therefore, the training set and model mismatch can be defined as $\mathcal{D} := \mathcal{D}_{dyn} \bigoplus \mathcal{D}_{kin}$, and $e(x_k, u_k) = x_{k+1} - f_{kin}(x_k, u_k)$. The differences between dynamic model and E-Kin model are only in the states ω and β, which means error e is of the form $[0, 0, 0, 0, 0, *, *]$, where $*$ is nonzero terms. For each state with nonzero error, we train a GP model of the form

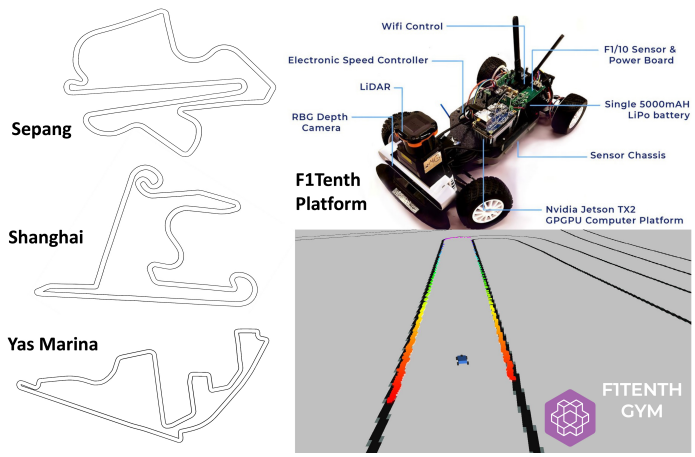

Figure 4: We use the ROS2 based F1TENTH Gym simulator (based on the F1Tenth Platform) in our work on three Formula One Tracks: Sepang International Circuit; Shanghai International Circuit; and Yas Marina Circuit

$$e_j := \mathcal{GP}(\omega, \beta, a, \triangle\delta), j \in \{6, 7\} \tag{8}$$

where j corresponds to the model mismatch in states ω and β, respectively. Specifically, $e_6 \sim \mathcal{N}(\mu_\omega, \sigma_\omega)$, and $e_7 \sim \mathcal{N}(\mu_\beta, \sigma_\beta)$

7 Results

We organize the evaluation processes of trained GP models in four categories: (i) Evaluation of GP models with different sample sizes, (ii) Evaluation on full track data with different scenarios settings, (iii) Evaluation of GP trained by sector track data, (iv) Evaluation of generalizability of GP model.

7.1 Evaluation metrics

To validate the performances of GP models, we use:

1. Model training time, $\mathcal{T}$;
2. Root mean square error, $RMSE$;
3. Coefficient of determination, R^2;

$$R^2(y, y^*) = 1 - \frac{\sum_{i=1}^{n}(y_i - y_i^*)^2}{\sum_{i=1}^{n}(y_i - \bar{y})^2} \tag{9}$$

where 1 is used to compare the time cost of GP models among different sample sizes, 2 and 3 are used to measure the performance of each GP model in model mismatch estimate.

7.2 Result1: Effect of kernel composing

Tracks	Size	RA_NON-CAP	CE_NON-CAP	RA_CAP	CE_CAP
Shanghai	Full	RQ + LINEAR	RQ + LINEAR	MATERN + LINEAR	RQ + LINEAR
	1/2	RQ + LINEAR	RQ × LINEAR	RBF×RQ	RQ×LINEAR
	1/3	RQ + LINEAR	RQ + LINEAR	RQ + LINEAR	RBF×RQ
Sepang	Full	RQ + LINEAR	RQ + LINEAR	RQ + LINEAR	MATERN + PERIODIC
	1/2	RQ + LINEAR	RQ + LINEAR	RQ + LINEAR	RQ×LINEAR
	1/3	RQ + LINEAR	RQ + LINEAR	RQ + LINEAR	RBF×RQ
Yas Marina	Full	MATERN + LINEAR	MATERN + PERIODIC	RBF×RQ	MATERN + PERIODIC
	1/2	RQ + LINEAR	RQ + LINEAR	RQ + LINEAR	MATERN + PERIODIC
	1/3	RQ + LINEAR	RQ + LINEAR	RQ + LINEAR	RBF×RQ

Table 4: Best kernel combination of each racing scenario on each racetrack. All kernels have been trained and tested in GPs with different sample sizes.

Kernel combination is a common solution for GP models that have different inputs, e.g. acceleration and steering velocity, in this paper. Here we present the full results of the best kernel combinations for vehicle modeling each scenario in different racetracks in Table 4. With all settings being the same, adding RQ and linear kernel functions produces the best GP model in most scenarios for GP trained on different sample sizes. We thus recommend: $RQ + LINEAR$ kernel is the overall most versatile combination for GP training for autonomous racing.

We also notice that the addition operation performs better than the multiplication operation. The kernels that multiply together tend to be difficult to converge in prediction as well as more time-consuming compared to adding kernels together. This may be because of the characteristics of these two operations [19]: (i) Adding kernels can be thought of as an OR operation, i.e., if you add together two kernels, then the resulting kernel will have a high value if either of the two base kernels has a high value. (ii) Multiplying two kernels can be considered an AND operation. That is, if you multiply together two kernels, then the resulting kernel will have a high value only if both of the two base kernels have a high value.

7.3 Result 2: Effect of sample size on GP

We evaluate the performance of GPs with different sample sizes in training time cost and prediction accuracy aspects.

The details of sample sizes for different simulation settings have been shown in Table 5. We evaluate the effect of global approximations of GP on training time and prediction accuracy. According to

Tracks \ Scenarios		RA_NON-CAP	CE_NON-CAP	RA_CAP	CE_CAP
Shanghai	training	2993	3042	2563	2780
	testing	3026	3079	3234	3345
Sepang	training	2838	3020	2597	2688
	testing	2738	2765	3083	3204
Yas Marina	training	2412	2543	2563	2468
	testing	2632	2662	2524	2600

Table 5: Training and testing data sample size of each track under different racing scenarios

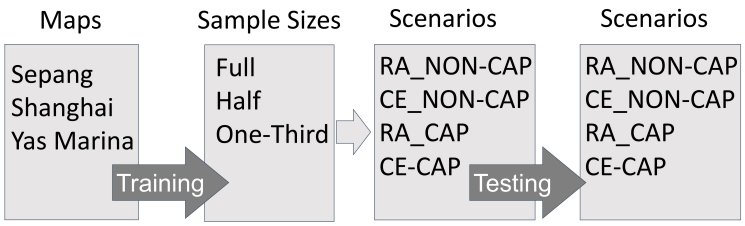

Figure 5: Evaluation of the best racing scenarios

Table 6, half-sized downsampling of the data can save around 70% training time, and one-third of full size can reduce up to 93% of the full-sized data training time.

Tracks	Size	RA_NON-CAP	CE_NON-CAP	RA_CAP	CE_CAP
Shanghai	Full	256.7	313.88	150.16	69.28
	1/2	65.81	58.35	28.68	32.98
	1/3	34.31	33.12	13.48	14.9
Sepang	Full	314.57	239.97	158.59	114.99
	1/2	58.74	38.55	30.46	32.98
	1/3	26.19	20.85	14.02	14.9
Yas Marina	Full	201.37	245.2	121.21	75.21
	1/2	38.66	47.49	31.5	18.4
	1/3	17.48	18.63	8.26	12.05

Table 6: Average training time of GPs with different sample sizes. Training time (in seconds) has been calculated in different scenarios across different racetracks.

Table 7 presents the prediction performance, which has shown that compared with full-sized GPs, training GPs with 50% less data only decreases model accuracy by 2%. Moreover, training with 66% less data only decreases the accuracy by 4%.

The global approximations of GP models can significantly reduce the time cost of training processes while remain good performance in the meantime. Therefore, if time is limited, we recommend using half or less data to train GP models.

7.4 Result 3: Effect of racing scenarios on GP

To evaluate the generalizability of different scenarios, we design the workflow as shown in Fig. 5. The training process is as same as before, but we compose a larger test set consisting of full-sized data sample and all the racing scenarios. Besides, we use the kernel combination yields the best performance of each scenario for testing.

As shown in Table 8, a dynamic speed reference is preferred since they always generalize better than the ones with fixed speed, and fixed speed profiles tend to cause high uncertainty. In addition, results also show that there are no significant benefits between the raceline and centerline. The centerline

Tracks	Size	RA_NON-CAP	CE_NON-CAP	RA_CAP	CE_CAP
Shanghai	Full	0.979	0.989	0.975	0.973
	1/2	0.965	0.976	0.965	0.968
	1/3	0.953	0.954	0.944	0.951
Sepang	Full	0.978	0.989	0.977	0.981
	1/2	0.977	0.981	0.975	0.968
	1/3	0.972	0.95	0.963	0.951
Yas Marina	Full	0.971	0.962	0.951	0.952
	1/2	0.958	0.938	0.95	0.947
	1/3	0.941	0.926	0.932	0.921

Table 7: Performance downgrade of global approximations of GP models. The value is calculated by mean values of explaining variances under different scenarios of each racetrack.

Tracks	Size	RA_NON-CAP	CE_NON-CAP	RA_CAP	CE_CAP
Shanghai	Full	0.988	0.989	0.982	0.983
	1/2	0.988	0.987	0.981	0.983
	1/3	0.984	0.985	0.969	0.972
Sepang	Full	0.991	0.991	0.963	0.968
	1/2	0.99	0.989	0.955	0.960
	1/3	0.984	0.981	0.950	0.951
Yas Marina	Full	0.963	0.965	0.961	0.953
	1/2	0.954	0.956	0.945	0.939
	1/3	0.912	0.923	0.917	0.867

Table 8: Performance of the best GP models of each scenario over the whole test set.

of a racetrack is easier to obtain, while the raceline, on the other hand, requires extra calculations of either minimal lap time or the shortest path. Therefore, using a dynamic speed profile with a centerline track file is sufficient for training a decent GP model.

7.5 Result 4: In-depth sectors analysis

We provide an in-depth analysis of local approximations, where we select three sectors of each racetrack and trained the GPs based on them.

Tracks	Sectors	RA_NON-CAP	CE_NON-CAP	RA_CAP	CE_CAP
Shanghai	1	0.888	0.973	-1.57e+09	-4.106e+20
	2	0.979	0.98	-5.01e+10	0.566*
	3	0.986	0.987	0.984	0.989
Sepang	1	0.975	0.904	-8.94	0.566*
	2	0.989	0.976	-5.316e+12	0.983*
	3	0.991	0.99	0.984	0.983
Yas Marina	1	0.903	0.874	0.955*	0.92*
	2	0.918	0.899	0.865*	0.78*
	3	0.959	0.942	0.961	0.935

Table 9: In-depth sectors analysis. Performance comparison among sectors under different scenarios of each racetrack. ($*$ denotes models with high uncertainty.)

One of our hypotheses is that a curve trajectory is better suited for training GPs than a straight trajectory where there is little variation in the data, i.e., yaw rate, ω and body slip angles, β. Therefore, in addition to the global approximations, we evaluate GPs on local subset of data. Specifically, we focus on three sectors of each racetrack. Fig. 6 shows chosen sectors of Yas Marina Circuit. To introduce the path variation, these sectors are composed of: (i) straight lines, where the error terms, e_ω, e_β, are almost constant; (ii) straight line with minor steering, causes a little variation in the error terms; (iii) curvy paths and cornering, which fluctuate error terms, e_ω and e_β. Although the training processes are conducted on local subsets, the test sets are full-sized data for each experiment. The kernel combination has been selected to be the best kernel for corresponding settings. Based on Table 9, the local approximations-based GP models yield accurate results as long as we select the correct representations. Specifically, GP models trained by curvy trajectories always have better prediction performances comparing to straight sectors. Besides, sector-trained GPs with CAP speed profile on straight trajectories tend to cause high model uncertainties. This also explains that why previous work of GP regression in vehicle dynamics modeling prefers to conduct experiments with artificial racetracks which seldom conclude straight line trajectories.

7.6 Result 5: Generalizing local approximations

We next evaluate the generalizability of local approximated GP models by testing them on racetracks other than the one used to train the models. In other words, we test the GP models trained on sectors on new racetracks that they have never seen. As the results shown in Table 9 indicates that GP regression models trained on curvier sectors always performs better than less curvy and straight

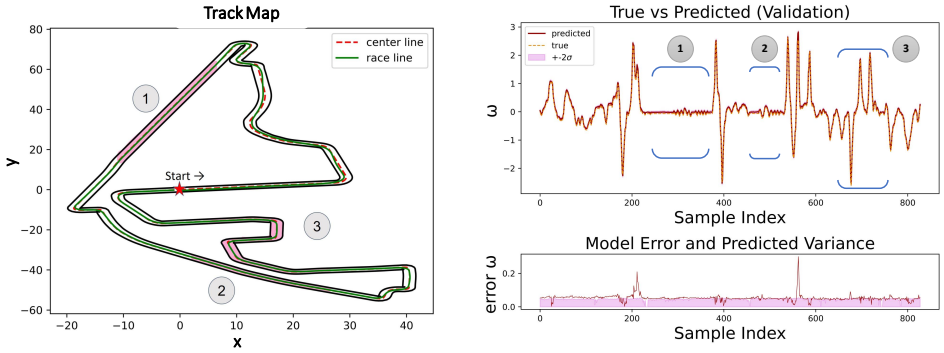

(a) (b)

Figure 6: Sector analysis: (a)three sectors of racetrack Yas Marina. (b) GP model predictions of corresponding sectors.

Tracks	Testing tracks	RA_NON-CAP	CE_NON-CAP	RA_CAP	CE_CAP
Shanghai	Sepang	0.989	0.99	0.989	0.987
	Yas Marina	0.962	0.943	0.965	0.95
Sepang	Shanghai	0.982	0.984	0.975	0.98
	Yas Marina	0.946	0.921	0.961	0.937
Yas Marina	Sepang	0.991	0.991	0.99	0.987
	Shanghai	0.987	0.989	0.981	0.986

Table 10: Sectors Generalization. In each racetrack, we train GP models on a local subset of the track using raceline + dynamic speed profile and test models on the other racetracks they have never seen.

sectors. Therefore, we select the third sector from each racetrack with combination of raceline and dynamic speed profile in the evaluation processes.

Based on Table 10, GP models trained on sectors generalize well across racetracks they have never seen. Noted we use the best kernel combinations of each racing scenario for this evaluation process. Although the sector-trained GP perform slightly worse, $2\% - 5\%$, than the full-sized models in prediction accuracy, they are much more computing efficient and can save 90% of the training time than full-sized GP models.

8 Conclusion and Discussion

In this paper, we implement a pure pursuit controller on the 1/10 scale racecar in a gym environment to drive on three real-world racetracks for data collection and then train GP regression models to learn model mismatch between single-track and extended kinematic models. Besides, we present a thorough study of vehicle dynamics modeling for autonomous racing using Gaussian Processes. For modeling evaluation, we have conducted the following experiments: (i) evaluation of kernel composing; (ii) evaluate the effect of global approximations; (iii) evaluate the effect of racing scenarios; (iv) an in-depth sectors analysis of each racetrack; (v) evaluation of the generalizability of each sector; (vi) limitation of GP regression models in small value data.

In the future, we will continue on evaluating the importance of GP models in vehicle dynamic modeling. We plan to implement advanced control algorithms on the corrected model: $f_{corr}(x_k, u_k) = f_{kin}(x_k, u_k) + e(x_k, u_k)$.By comparing the control performance between corrected vehicle models and real dynamics models, we will clearly understand the capability of GP regression in vehicle dynamic modeling for autonomous racing.

References

[1] Gabriel Hartmann, Zvi Shiller, and Amos Azaria. Autonomous head-to-head racing in the indy autonomous challenge simulation race. *arXiv preprint arXiv:2109.05455*, 2021.

[2] Varundev Suresh Babu and Madhur Behl. f1tenth. dev-an open-source ros based f1/10 autonomous racing simulator. In *2020 IEEE 16th International Conference on Automation Science and Engineering (CASE)*, pages 1614–1620. IEEE, 2020.

[3] Jesús Velasco Carrau, Alexander Liniger, Xiaojing Zhang, and John Lygeros. Efficient implementation of randomized mpc for miniature race cars. In *2016 European Control Conference (ECC)*, pages 957–962. IEEE, 2016.

[4] Matthew O'Kelly, Varundev Sukhil, Houssam Abbas, Jack Harkins, Chris Kao, Yash Vardhan Pant, Rahul Mangharam, Dipshil Agarwal, Madhur Behl, Paolo Burgio, et al. F1/10: An open-source autonomous cyber-physical platform. *arXiv preprint arXiv:1901.08567*, 2019.

[5] Alexander Wischnewski, Maximilian Geisslinger, Johannes Betz, Tobias Betz, Felix Fent, Alexander Heilmeier, Leonhard Hermansdorfer, Thomas Herrmann, Sebastian Huch, Phillip Karle, et al. Indy autonomous challenge-autonomous race cars at the handling limits. In *12th International Munich Chassis Symposium 2021*, pages 163–182. Springer, 2022.

[6] Matthias Althoff and Silvia Magdici. Set-based prediction of traffic participants on arbitrary road networks. *IEEE Transactions on Intelligent Vehicles*, 1(2):187–202, 2016.

[7] Juan-Bautista Tomas-Gabarron, Esteban Egea-Lopez, and Joan Garcia-Haro. Vehicular trajectory optimization for cooperative collision avoidance at high speeds. *IEEE Transactions on Intelligent Transportation Systems*, 14(4):1930–1941, 2013.

[8] Achin Jain, Matthew O'Kelly, Pratik Chaudhari, and Manfred Morari. Bayesrace: Learning to race autonomously using prior experience. *arXiv preprint arXiv:2005.04755*, 2020.

[9] Sebastian Thrun, Mike Montemerlo, Hendrik Dahlkamp, David Stavens, Andrei Aron, James Diebel, Philip Fong, John Gale, Morgan Halpenny, Gabriel Hoffmann, et al. Stanley: The robot that won the darpa grand challenge. *Journal of field Robotics*, 23(9):661–692, 2006.

[10] Jason Kong, Mark Pfeiffer, Georg Schildbach, and Francesco Borrelli. Kinematic and dynamic vehicle models for autonomous driving control design. In *2015 IEEE intelligent vehicles symposium (IV)*, pages 1094–1099. IEEE, 2015.

[11] Matthias Althoff, Markus Koschi, and Stefanie Manzinger. Commonroad: Composable benchmarks for motion planning on roads. In *2017 IEEE Intelligent Vehicles Symposium (IV)*, pages 719–726. IEEE, 2017.

[12] Rajesh Rajamani. *Vehicle dynamics and control*. Springer Science & Business Media, 2011.

[13] Jeong Hwan Jeon, Sertac Karaman, and Emilio Frazzoli. Anytime computation of time-optimal off-road vehicle maneuvers using the rrt. In *2011 50th IEEE Conference on Decision and Control and European Control Conference*, pages 3276–3282. IEEE, 2011.

[14] Zvi Shiller, Yu-Rwei Gwo, et al. Dynamic motion planning of autonomous vehicles. *IEEE Transactions on Robotics and Automation*, 7(2):241–249, 1991.

[15] Lukas Hewing, Alexander Liniger, and Melanie N Zeilinger. Cautious nmpc with gaussian process dynamics for autonomous miniature race cars. In *2018 European Control Conference (ECC)*, pages 1341–1348. IEEE, 2018.

[16] Alexander Wischnewski, Johannes Betz, and Boris Lohmann. A model-free algorithm to safely approach the handling limit of an autonomous racecar. In *2019 IEEE International Conference on Connected Vehicles and Expo (ICCVE)*, pages 1–6. IEEE, 2019.

[17] Finn Lukas Busch, Jake Johnson, Edward L Zhu, and Francesco Borrelli. A gaussian process model for opponent prediction in autonomous racing. *arXiv preprint arXiv:2204.12533*, 2022.

[18] Tim Brüdigam, Alexandre Capone, Sandra Hirche, Dirk Wollherr, and Marion Leibold. Gaussian process-based stochastic model predictive control for overtaking in autonomous racing. *arXiv preprint arXiv:2105.12236*, 2021.

[19] David Duvenaud. *Automatic model construction with Gaussian processes*. PhD thesis, University of Cambridge, 2014.

[20] Haitao Liu, Yew-Soon Ong, Xiaobo Shen, and Jianfei Cai. When gaussian process meets big data: A review of scalable gps. *IEEE transactions on neural networks and learning systems*, 31(11):4405–4423, 2020.

[21] Matthew O'Kelly, Hongrui Zheng, Dhruv Karthik, and Rahul Mangharam. F1tenth: An open-source evaluation environment for continuous control and reinforcement learning. In *NeurIPS 2019 Competition and Demonstration Track*, pages 77–89. PMLR, 2020.

[22] R Craig Coulter. Implementation of the pure pursuit path tracking algorithm. Technical report, Carnegie-Mellon UNIV Pittsburgh PA Robotics INST, 1992.

[23] Fabian Christ, Alexander Wischnewski, Alexander Heilmeier, and Boris Lohmann. Time-optimal trajectory planning for a race car considering variable tyre-road friction coefficients. *Vehicle system dynamics*, 59(4):588–612, 2021.